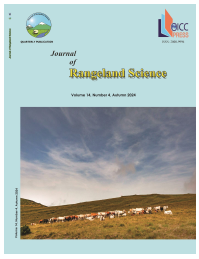

Volume 14, Issue 4, 142431 (1-11)

Journal of Rangeland Science (JRS)

https://dx.doi.org/10.57647/j.jrs.2024.1404.31

Spatio-temporal assessment of meteorological droughts effect on vegetation droughts in Khorasan Razavi province, Iran

Pouyan Dehghan Rahimabadi, Sahar Nasabpour Molaei, Esmaeil Heydari Alamdarloo, Setareh Bagheri, Hossein Azarnivand*

Faculty of Natural Resources, University of Tehran, Tehran, Iran.

*Corresponding author: hazar@ut.ac.ir

Research and Full Length Article

Received:
21 April 2023
Revised:
21 September 2023
Accepted:
31 October 2023
Published online:
15 October 2024

Abstract:

Vegetation cover is one of the living components of terrestrial ecosystems and plays an important role in many ecosystem processes that are strongly influenced by climatic events. Thus, meteorological droughts can significantly affect the vegetation cover, especially in arid and semi-arid regions where vegetation is more sensitive to environmental conditions. This study was conducted with the aim of analyzing the effects of meteorological droughts on the vegetation cover in different Land Use Land Cover (LULC) types in Khorasan Razavi province, Iran. For this purpose, the correlation and Linear Regression (LR) between Standardized Vegetation Index (SVI) and meteorological drought indices including Standardized Precipitation Index (SPI) and Standardized Precipitation Evapotranspiration Index (SPEI), with 3, 6 and 12-month time scales were investigated for the period of 2001 – 2020. Based on the results, it was found that SVI values were negative in the years 2001, 2006, 2008, 2011, 2014 and 2015, in all LULC types while in 2010, moderate rangeland experienced the most severe drought. The decreasing trend of SVI (increasing vegetation drought) was mostly observed in the southern parts of the province. The correlation between SVI and 6- month SPEI occupied a wider area than the other time scales (23.07%). The highest correlation between SVI and 12-month SPI was distinguished in dense forest, sparse forest, and poor rangeland, and occupied a wider area across the province (24.08%). Moreover, the highest (1.13) and lowest (0.75) changes in the regression coefficient of variations of SVI with multitemporal SPEI and SPI were belonged to moderate forest and agricultural land, respectively. Based on the results of this study, SPEI and SPI showed completely different values in various LULC types. Therefore, any types of indicators should be separately considered to study the terrestrial ecosystems in order to better identify areas affected by meteorological drought.

Keywords: Climate; Drought; Indicator; Trend; Vegetation

Introduction

Vegetation cover provides valuable ecosystem services to various terrestrial ecosystems such as carbon sequestration, livestock grazing and regulation of water resources (Pakeman et al., 2019). It is predicted that future climate warming will have a great impact on terrestrial ecosystems including rangeland degradation and desertification (Miao et al., 2015), increasing tree mortality, stimulating fires in ecosystems and reducing carbon sequestration in vegetation cover (Allen et al., 2010). Therefore, drought can be an important factor in the quantity and quality of vegetation (Zandi et al., 2021). A shift towards more variable rainfall leads to an overall reduction in the forage biomass resources and an increase in the vegetation cover vulnerability (Williams and Albertson, 2006). Hence, quantifying the vegetation cover response to meteorological droughts is essential for ecological management in terrestrial ecosystems (Wei et al.,

2022). However, it is difficult to predict and quantify meteorological drought because it is a complex phenomenon, appears gradually, does not have a specific beginning and is affected by numerous variables. That is why the characteristics of drought, its intensity and frequency are spatially and temporarily different (Iglesias et al., 2009). Different terrestrial and meteorological parameters are important for the drought parameterization. Because the global air temperature is continuously increasing affected by climate change and the spatio- temporal pattern of rainfall and land use is expected to change significantly in the coming decades (Liu et al., 2014). Therefore, it is necessary to develop the most accurate and effective drought monitoring tools. In this case, Remote Sensing (RS) plays an important role in drought studies, due to the spatial and temporal advantages it can provide (West et al., 2019).

Meteorological drought monitoring and the evaluation of its impact on vegetation cover is essential for proper management of terrestrial ecosystems. Traditionally, this goal has been achieved by the direct use of meteorological drought indices which is calculated from *in situ* observation data collected at a limited number of meteorological stations. While these indices are accurate, they are not capable of providing spatially accurate drought estimates due to geographic and economic constraints when establishing *in situ* stations (Ozelkan et al., 2016). However, todays, there are different indicators for drought diagnosing and monitoring in real time (Ghazaryan et al., 2020), announcing the beginning or end of the drought (Tarnavsky and Bonifacio, 2020), studying drought levels and drought response measures (Zargar et al., 2011), analyzing the quantitative effects of droughts on environmental variables at a various spatial and temporal scales (Tarnavsky and Bonifacio, 2020) and finally announcing drought conditions (Adedeji et al., 2020; Tsakiris and Vangelis, 2004) and using in drought warning, monitoring and contingency planning.

Several methods have been used to monitor and evaluate meteorological droughts and their effects on vegetation cover, through the development of various climatic and vegetation indices based on RS techniques. Ariapour et al. (2013) estimated the changes in vegetation cover and Land Use Land Cover (LULC) using Landsat TM and ETM$^+$ images in Sabzevar city, Iran. The results indicated the appropriateness of RS technology in order to accurately estimate the area of LULC and vegetation changes was confirmed by these researchers. Ezzine et al. (2014) investigated the consistency of three drought indices in different LULC classes during a 15- year period (1998-2012). Their results showed a stronger relationship between Standardized Precipitation Index (SPI) and Standardized Vegetation Index (SVI) than SPI and Standardized Water Index (SWI) in autumn and winter seasons. Su et al. (2017) proposed a framework of standard drought indicators to describe all aspects of drought, duration, onset, intensity, expansion and simultaneous examination of three types of drought such as agricultural, meteorological and hydrological droughts in order to harmonize the drought monitoring and reduce the contradictions caused by the lack of a global standard for measuring and describing drought. Shad et al. (2017) investigated the drought in Isfahan province, Iran, using SPI, Temperature Condition Index (TCI), Vegetation Condition Index (VCI) and Normalized Difference Vegetation Index (NDVI). The results of the correlation among different drought indices showed that VCI and TCI have the highest and lowest correlations with meteorological droughts, respectively. Alamdarloo et al. (2021) investigated the effect of climate fluctuations on vegetation dynamics in Northwest of Iran. They reported that NDVI had the positive correlation with temperature in 8°-12 °C class with R^2 value of 0.36 and precipitation in 213 – 300 mm classes with a R^2 value of 0.38. Khusfi and Zarei (2020) assessed the relationship between meteorological droughts and vegetation degradation using SPI and NDVI in the Meyghan plain in Markazi province, Iran. They reported that the decrease in precipitation increased the sensitivity of the low density vegetation cover (poor rangeland) to meteorological droughts compared to dense vegetation cover (agricultural land).

Considering the above and emphasizing the dangers of droughts, it is necessary to realize the relationship between vegetation cover and meteorological drought to understand the effects of water scarcity on vegetation production and initiate prevention. Since Khorasan Razavi province, in northeast of Iran, has been introduced as one of the drought-prone regions in the country, which suffers a lot of damage due to this phenomenon every year (Erfanian and Alizadeh, 2009), this study aimed to investigate the meteorological drought in this province, using SPEI and SPI and their effect on vegetation cover in different LULC types. In this study, both SPEI and SPI were used to assess the effect of each of them on vegetation cover and compared their effects.

Materials and methods

Study area

The case study is in Khorasan Razavi province (33°52′-37°52′ N; 56°19-61°16′ E), located in the northeast of Iran, with an area of 127,222 Km^2. About three fourth of the province is dominated by arid and semi-arid climates. The average annual rainfall is 250 mm, which changes from 116 in the north to 313 mm in the south and the annual mean temperature is about 14.5°C (www.irimo.ir). Moreover, the altitude varies between 231 and 3308 m above sea level (Figure 1).

Land use land cover

Land Use Land Cover (LULC) was used to represent the effect of meteorological drought on dynamics of different types of vegetation cover. In this study, LULC map was extracted from the LULC map prepared by Natural Resources and Watershed Management Organization of Iran (www.frw.ir). This map was divided LULC into 13 types including dense forest (3.78%), moderate forest (0.12%), sparse forest (1.44%), agricultural land (24.78%), good rangeland (2.49%), moderate rangeland (21.17%), poor rangeland (37.73%), bareland (2.51%), rock (0.48%), salt land (2.62%), sand dune (2.14%), urban (0.41%), wetland (0.33%) (Figure 2).

Methodology

In the present study, Standardized Vegetation Index (SVI) was adopted to represent the vegetation cover dynamics. SVI maps prepared using the monthly Enhanced Vegetation Index (EVI) acquired from MOD 13A2 product of MODIS for the period of 2001 – 2020. EVI maps for May were used because the natural vegetation cover is at its peak on this month in Khorasan Razavi province. Additionally, the monthly precipitation and temperature data for 10 synoptic stations existing in the study area within the period of 2000-2020 were used (Table 1). Two of the most widely used meteorological drought indices including Standardized Precipitation Evapotranspiration Index (SPEI) and Standardized Precipitation Index (SPI) were calculated to characterize the intensity of meteorological drought. The 3, 6 and 12- month SPEI and SPI were considered as short, medium and long time scales, respectively. Afterwards, coefficient of determination (R^2) and regression coefficient between SVI and multitemporal SPEI and SPI to assess the relationship between vegetation cover dynamics and meteorological droughts. The maximum value of the R^2 for each pixel was considered to evaluate the response of SVI to different SPEI and SPI time scales. This means that if a pixel of the SVI maps showed the best correlation with the 3- month SPEI, cumulative precipitation and reference evapotranspiration from February was computed. It should be noted that the response of vegetation cover to meteorological droughts were analyzed and compared with a 20-year period in seven LULC types including dense forest, moderate forest, sparse forest, good rangeland, moderate rangeland, poor rangeland and agricultural land. The bareland, rock, saltland, sand dune, urban, and wetland classes were considered no- vegetation types and masked in the results.

Standardized vegetation index (SVI)

The SVI is used to monitor the vegetation cover dynamics. In this study, EVI maps were used to generate SVI

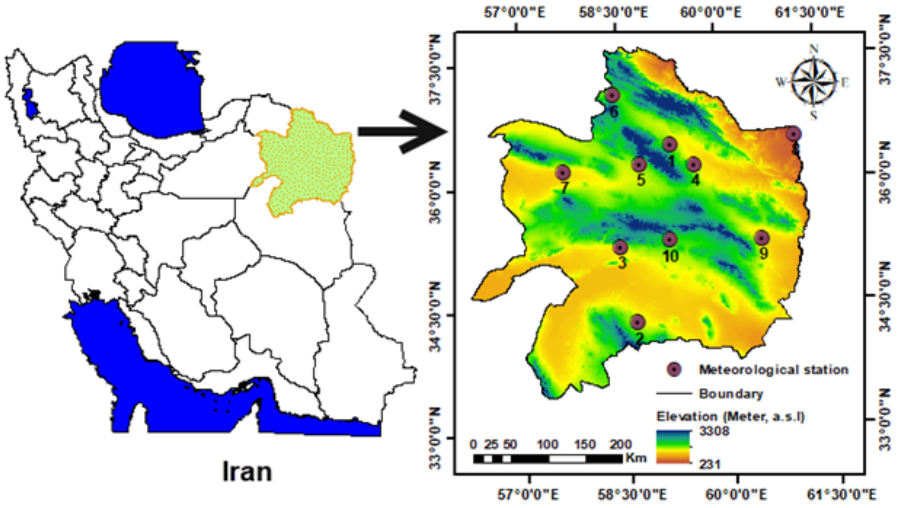

Figure 1. Geographical location of Khorasan Razavi province in Iran and the distribution of synoptic stations.

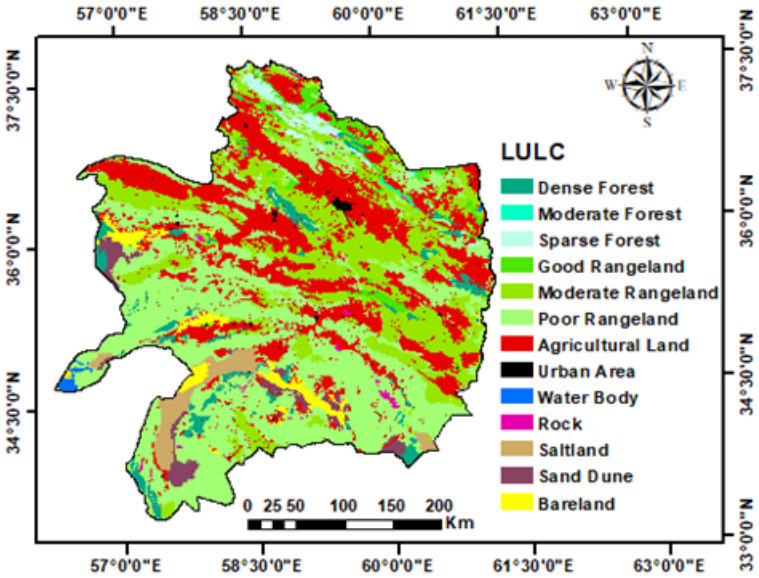

Figure 2. Land Use Land Cover map of Khorasan Razavi province.

Table 1. The properties of the synoptic stations.

Row	Station Name	Longitude (E)	Latitude (N)	Altitude (m)	Mean Annual Precipitation (mm)	Mean Monthly Temperature (°C)
1	Golmakan	36.48	59.28	1176.00	212.28	15.97
2	Gonabad	34.35	58.68	1056.00	116.27	18.62
3	Kashmar	35.27	58.47	1109.70	177.44	18.42
4	Mashhad	36.24	59.63	999.20	232.29	15.85
5	Neyshabur	36.27	58.8	1213.00	229.67	14.85
6	Quchan	37.10	58.45	1287.00	325.97	12.46
7	Sabzevar	36.21	57.65	962.00	180.27	18.14
8	Sarakhs	36.54	61.15	977.60	192.28	18.50
9	Torbat-E-Jam Torbat-E	35.29	60.56	950.40	157.25	16.27
10	Heydariyeh	35.33	59.21	1451.00	225.22	14.64

maps. EVI is a more robust proxy for biomass due to its improved resistance to soil and atmospheric contamination, compared to NDVI (Huete et al., 2002; Matsushita et al., 2007; Garroutte et al., 2016). SVI describes the probability of variation of the normal EVI over the time, in a certain interval (Veneros and García, 2022). This index was computed for each pixel as Equation (1):

$$\mathrm{SVI} = \frac{\mathrm{EVI}_i - \mathrm{EVI}_{mean}}{\mathrm{STD}} \tag{1}$$

where;
SVI is Standardized Vegetation Index,
EVI_i is Enhanced Vegetation Index for month i (May) and
EVI_{mean} is mean value of EVI in May during 2001 – 2020 and
STD is standard deviation of EVI in May during 2001 – 2020.
After calculating SVI for the years 2001 to 2020, Mann-Kendall test was used to detect the vegetation cover trend (Mann, 1945; Kendall, 1975).

Precipitation evapotranspiration index

SPEI is an extended form of SPI. This index is developed to consider precipitation and potential evapotranspiration in determining meteorological drought. Unlike SPI, SPEI shows the main effect of increase in temperature on water demand. Thus, SPEI is an appropriate index to assess the intensity of drought in the increasing global warming (Vicente-Serrano et al., 2010). In this study, the monthly SPEI was calculated to determine the climate change trends to investigate the response of vegetation to climate change using precipitation and potential evapotranspiration data.
To estimate potential evapotranspiration, Thornthwaite (1948) equation was used as: N_m is the correction coefficient that is determined based on the month and the latitude of the studied area,
T_m is the average temperature of the month in °C,
I is thermal index calculated for the whole year and
α is a coefficient computed based on I.
Next, the monthly water deficit or surplus Equation (2)

$$\mathrm{PET} = 16N_m\left(\frac{10T_m}{I}\right)^{\alpha} \tag{2}$$

where;

$$D_i = P_i - PET_i$$

is computed and after that, X_{ij}^k is calculated as Equation (3).

$$X_{ij}^k = \begin{cases} \sum_{l=13-k+j}^{12} D_{i-1l} + \sum_{l=1}^{j} D_{ij} & if \quad j < k \\ \sum_{l=j-k+1}^{j} D_{ij} & if \quad j \geq k \end{cases} \tag{3}$$

where;
i is the respective year,
j is the respective month and
k is time scale (k= 3, 6 and 12).
In order to standardize the series of water deficit or surplus observations to determine SPEI according to Vicente-Serrano et al. (2013), three- factor log- logistic distribution was used as the most appropriate adaptive distribution based on Equation (4):

$$f(x) = \frac{\beta}{\alpha}\left(\frac{x-Y}{\alpha}\right)^{\beta-1}\left[1+\left(\frac{x-Y}{\alpha}\right)\right]^{-2} \tag{4}$$

where;
α, β, and Y are scale, shape, and boundary factors, respectively,
For D values in the interval $Y < D < \infty$. Also, Equation (5) shows the probability distribution function of the observation series of water deficit or surplus according to the log-logistic distribution.

$$F(x) = \left[1+\left(\frac{x-Y}{\alpha}\right)^{\beta}\right]^{-1} \tag{5}$$

Eventually, based on $F(x)$, the SPEI was computed as Equation (6):

$$SPEI = W - \frac{C_0 + C_1 W + C_2 W^2}{1 + d_1 w + d_2 w^2 + d_3 w^3} \tag{6}$$

where;
C_0=2.515517, C_1=0.802853, C_2=0.010328, d_1=1.432788, d_2=0.18926 and d_3=0.001308, which are constants.

$$W = \sqrt{-2\ln P}$$

P= represents precipitation.
if *P*=1-*F(x)* ≤0.5 but if *P* >0.5, P was replaced by 1-*P*,
SPEI has positive and negative values, the most negative value indicates the more drought intensity and the positive values represent a wet condition.

Standardized precipitation index

SPI was computed with monthly precipitation data for the period of 2000–2020 to assess the intensity of meteorological drought. To calculate the SPI, the precipitation data for each station should be fitted to the gamma probability distribution function. The probability density function of this distribution is given in Equation (7) (McKee et al., 1993):

$$g(x) = \frac{1}{\beta^{\alpha}\Gamma(\alpha)} x^{(\alpha-1)e^{\frac{-x}{\beta}}} \quad for \quad x > 0 \qquad (7)$$

where;
x is the amount of precipitation,
α is the shape parameter,
β is the scale parameter, and
$\Gamma(\alpha)$ represents the gamma function.
It should be noted that x, α and β values must be greater than zero.
α and β are calculated using Equations (14), (15) and (16):

$$\alpha = \frac{1}{4A}\left(1 + \sqrt{1 + \frac{4A}{3}}\right) \qquad (8)$$

$$\beta = \frac{\bar{x}}{4A} \qquad (9)$$

$$A = \ln(\bar{x}) - \frac{\sum \ln(\bar{x})}{n} \qquad (10)$$

where;
n is the number of observed precipitations. In addition,
$\bar{x}$is the average cumulative precipitation for a month during the statistical period.
The calculated parameters allow the precipitation distribution in the station to be effectively represented by a mathematical cumulative probability function according to Equation 11:

$$G(x) = \int_0^x \frac{1}{\beta^{\alpha}\Gamma(\alpha)} \int_0^x x^{\alpha-1} e^{\frac{-x}{\beta}} dx \qquad (11)$$

Since the gamma function is not defined for the values of x = 0 and the precipitation distribution may take a zero value, the cumulative probability is obtained using Equation (12):

$$H(x) = q + (1-q)G(x) \qquad (12)$$

where;
q is the probability of zero and
H(x) is the cumulative probability function with x = 0 data. Then, it is transformed into a standard normal distribution to produce the cumulative SPI values of *H(x)* (McKee et al., 1993).

Calculation of coefficient of determination (R^2) and linear regression coefficient

Using the R^2, the correlation of SVI in relation to multitemporal SPEI and time was calculated according to Equation (13):

$$R^2 = 1 - \frac{RSS}{TSS} \qquad (13)$$

where;
R^2 is coefficient of determination and
RSS is Residuals Sum of Squares
TSS is Total Sum of Squares,
The R^2 values ranges from 0 to 1, which higher values represent better agreement between the compared data (Pogacar et al., 2022).
Additionally, LR analysis can be used to simulate the changes trends. The regression coefficient of the SVI changes in relation to multitemporal *SPEI* and SPI was determined using Equation (14):

$$b = \frac{n\sum_n^{i=1} x_i y_i - \sum_n^{i=1} x_i \sum_n^{i=1} y_i}{n\sum_n^{i=1} x_i^2 - (\sum_n^{i=1} x_i)^2} \qquad (14)$$

where;
X_i and Y_i are independent and dependent variable values in ith year, respectively, and
n represents the number of years during the study period (n=20). Generally, if,
b <0 reflects that the dependent variable has an increasing trend, while
b >0 reflects that the dependent variable shows a decreasing trend.
b =0 shows that the dependent variable has no trend.
The *SPEI* and SPI calculations were carried out and coded in MATLAB R2021b for each station on 3, 6 and 12-month time scales as short, medium and long- time scales, respectively. Then, they were interpolated across the study area using Inverse Distance Weighted (IDW) model in ArcMap 10.8.1 to obtain SPEI and SPI maps. The pixel size and position were considered as SVI maps. Moreover, the coefficient of determination and LR were conducted in TerrSet 2020 v.19.0.6. The flow chart of the procedure used in this study is shown in Figure 3.

Results

Trend of precipitation and temperature changes

Figure 4 illustrates the trend of changes in annual precipitation during 2000 – 2020 in Khorasan Razavi province. The results represented that the trend of variations in precipitation was generally increasing. In 2000, the annual precipitation was 153.00 mm, and it reached maximum value of 305.53 mm in 2020. Moreover, there was the lowest annual precipitation in 2008 (90.144 mm).
Figure 5 shows the trend of changes in annual temperature during 2000 – 2020 in Khorasan Razavi province. The results indicated that the trend of temperature variations was generally decreasing. The annual temperature was 16.6 °C in 2000 while it reached minimum value of 15.5 °C in 2020. Also, the highest mean temperature was 15.5 °C in 2001.

Trend of SVI

The occurrence and cessation of vegetation drought in different LULC types in Khorasan Razavi province over the past 20 years are presented in Figure 6. The lower SVI values indicate greater severity of agricultural drought. As it can be seen, in the years 2001, 2006, 2008, 2011, 2014 and 2015, the SVI values in all LULC types are negative, which

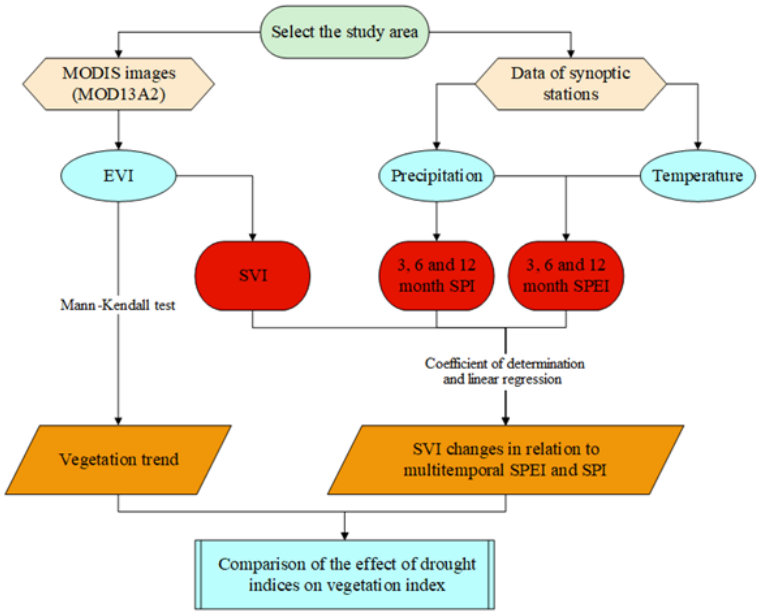

Figure 3. Flowchart of the procedure employed in this study

indicates that the vegetation is not in a good condition and drought affects all LULC types. While in 2010, moderate rangeland has experienced the most severe drought. The years 2019 and 2020 recorded the highest SVI values in all LULC types, which indicates the cessation of drought conditions and better vegetation status, which is related to the rainfall in the previous years.

The trend of SVI over the period of 2001-2020 in different LULC types and its relative percentage are presented in Figure 7 and Table 2, respectively. According to the analysis of the Mann Kendall trend test, large areas of Khorasan Razavi province were not under any drought trend (99.42%). The increasing trend of SVI (suitable condition of vegetation cover over time) was observed in a sporadically in the province. These pixels showed relief from drought conditions. On the other hand, the decreasing trend of SVI (reduction of vegetation cover or occurrence of drought) with the least number of pixels was observed in the southern part of the province.

According to the results presented in Table 2, the highest (23.67%) and the lowest (3.43%) relative percentages of the increasing trend of SVI belong to the moderate rangeland and moderate forest, respectively. Additionally, moderate forest had the highest relative percentage of the no-trend among other LULC types. The highest (1.08) and lowest (0.00) relative percentages of the decreasing trend were also observed in agricultural land and with the same value of moderate forest and sparse forest, respectively.

SVI-SPEI and SVI-SPI

The spatial distribution of the highest correlation between SVI and multitemporal SPEI and SPI is presented in Fig-

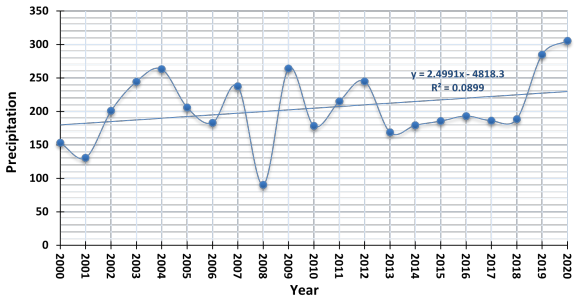

Figure 4. The trend of changes in annual precipitation during 2000 to 2020 in Khorasan Razavi province

Table 2. Relative percentage of SVI trend classes in different LULC types (%).

LULC Type	Decreasing Trend	No Trend	Increasing Trend
Dense Forest	0.49	79.74	19.77
Moderate Forest	0.00	96.57	3.43
Sparse Forest	0.00	76.18	23.82
Good Rangeland	0.01	86.00	13.99
Moderate Rangeland	0.10	76.23	23.67
Poor Rangeland	0.59	82.35	17.06
Agricultural Land	1.08	85.40	13.52
Total Area	0.58	81.67	17.75

ure 8. This map showed the response of agricultural drought to meteorological droughts. The correlation of SVI with 6-month SPEI had covered a wider area than other time scales (3 and 12-month). In other words, agricultural drought was associated with medium- term rainfall at the most regions. In fact, the distribution of agricultural drought severity had a strong relationship with this time scale of precipitation.

The area of effect of multitemporal SPEI and SPI of vegetation cover in different LULC types is presented in Table 3. The highest correlation value between SVI and 3, 6 and 12-month SPEI include 15.11%, 23.07% and 7.14%, respectively, while the highest correlation value between SVI and 3, 6 and 12-month SPI include 16.30%, 14.30% and 24.08% of the province, respectively.

The highest correlation between vegetation cover and 12-month SPI has been reported in dense forest, sparse forest, and poor rangeland. In other words, the 12-month time scale is more effective on the vegetation cover in poor rangeland than other time scales, and the vegetation is affected by long-term rainfall in this LULC type. On the other hand, the lowest correlation is observed in moderate forest and good rangeland in relation to 3-month SPEI. In other words, temperature and short-term rainfall affect the vegetation cover in these LULC types. Moderate rangeland and agricultural land are also affected by 6-month SPEI or medium-term temperature and precipitation.

Correlation of SVI-SPEI and SVI-SPI

The correlation rate of SVI and multitemporal SPEI and SPI is shown in different colors (Figure 9). In darker pixels (dark blue), the correlation is higher. Most of the pixels with these values are concentrated in the northeast and southwest. While the correlation of SVI and multitemporal SPEI and SPI is lower in brighter pixels (pale yellow). Pixels with these values are scattered throughout the region, especially in the southern parts. However, the sensitivity of vegetation cover to meteorological drought is more in the eastern sides and some areas in north, west and south sides than central, northwestern, southwestern and southeastern parts.

Regression of SVI-SPEI and SVI-SPI

The regression between SVI and multitemporal SPEI and SPI in presented in Figure 10. The regression coefficient of SVI changes in relation to multitemporal SPEI and SPI is higher in darker pixels than in brighter pixels. In fact,

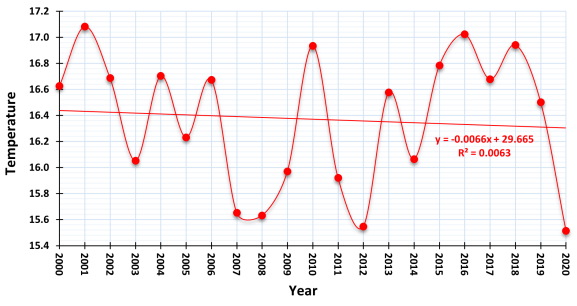

Figure 5. The trend of changes in annual temperature during 2000 to 2020 in Khorasan Razavi province.

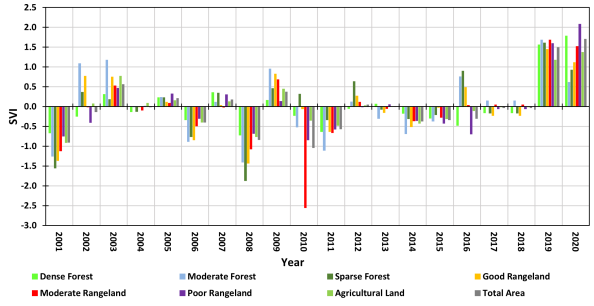

Figure 6. SVI variation in different LULC types over time.

the vegetation cover in darker pixels is more sensitive to meteorological drought or changing climate factors. So, the vegetation cover in these areas is more susceptible to the negative effects of meteorological drought. However, the spatial distribution of pixels with higher values does not follow a particular pattern, but it is less in west and southeast sides.

Table 4 represents R^2 and regression coefficient values between SVI and multitemporal SPEI and SPI in different LULC types. The highest (0.60) and lowest (0.37) R^2 of SVI with multitemporal SPEI and SPI are higher in moderate forest and agricultural land, respectively, than other LULC types. The highest (1.13) and lowest (0.75) regression coefficient of SVI changes in relation to SPEI and SPI also belong to moderate forest and agricultural land, respectively. Based on the results of this part, moderate forest has a higher correlation and sensitivity to meteorological drought and climate change. Reducing the sensitivity of agricultural land to climate fluctuations is also related to human activities such as land management and irrigation.

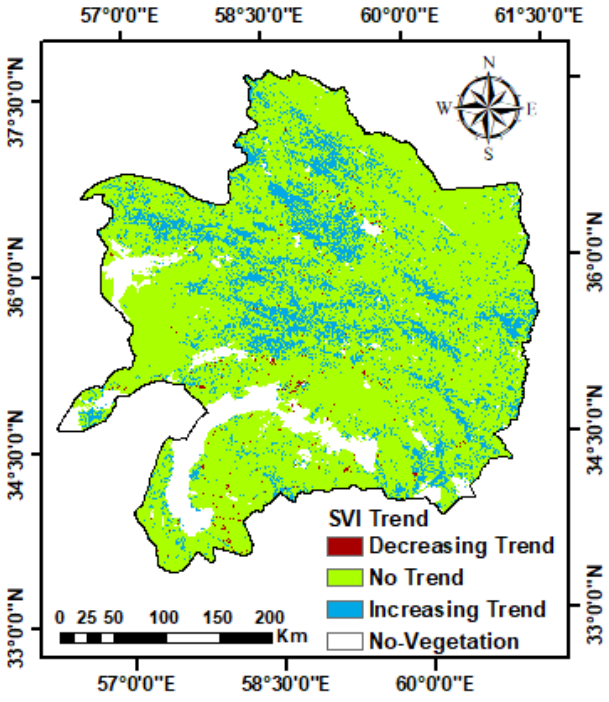

Figure 7. The trend of SVI changes.

Discussion and conclusion

In this study, multitemporal SPEI and SPI were used to investigate the recent meteorological drought in Khorasan Razavi province because both precipitation and temperature, as two most important meteorological factors, are used as an index to achieve a better understanding in the drought's evolution (McKee et al., 1993). The multitemporal feature of these indices made it possible to analyze different types of droughts in different time scales. Additionally, the dominant meteorological drought time scales in which drought affects vegetation cover, the extent and spatio-temporal characteristics of SPEI and SPI were investigated. Based on the results, in 2001, 2006, 2008, 2011, 2014 and 2015, SVI values are negative in all LULC types. While in 2010, moderate rangeland has faced the worst agricultural drought conditions in the region during the past 20 years. Therefore, it can be concluded that these LULC types experienced severe agricultural and meteorological droughts in 2010.

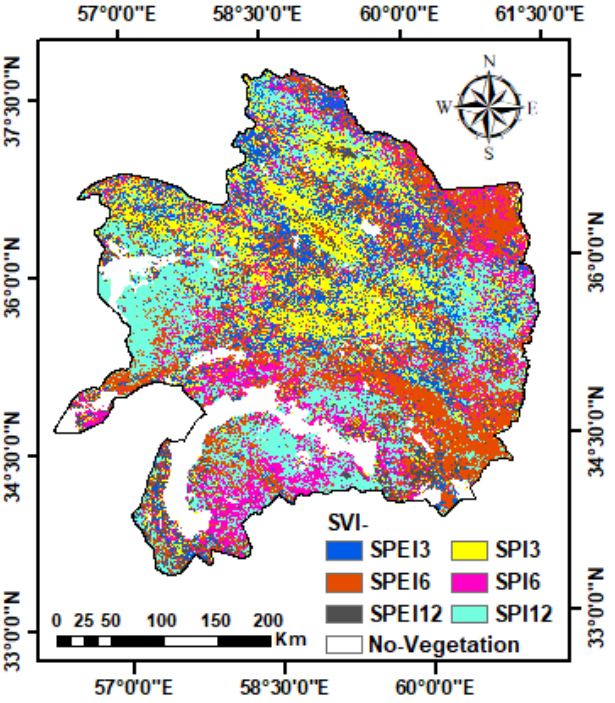

Figure 8. The highest correlation between SVI and 3, 6 and 12-month SPEI and SPI.

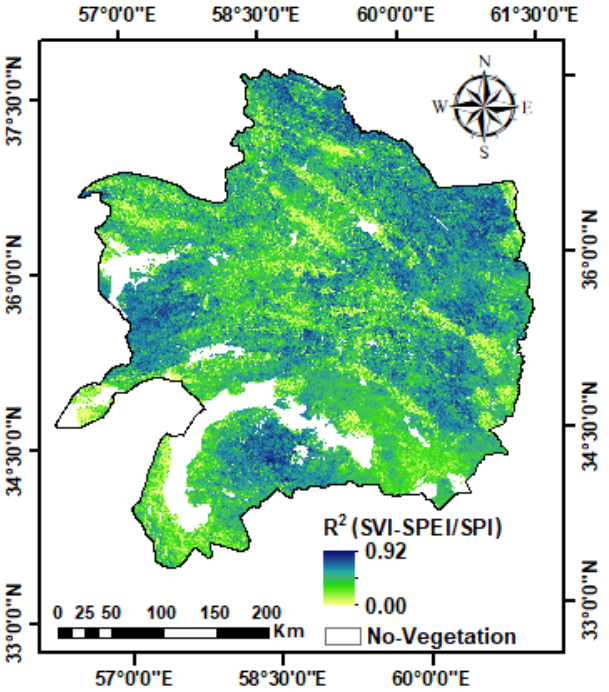

Figure 9. The R^2 between SVI and multitemporal SPEI and SPI.

It was also found that vegetation cover in large areas of Khorasan Razavi province is not affected by any drought increasing process. While the decreasing trend of SVI is mainly observed in the southern parts of the province. Therefore, it is essential to prioritize this part of the province to take any activities to deal with the drought.

In moderate forest and sparse forest, the highest relative percentage of decreasing trend is observed, which indicates that vegetation cover in these LULC types are most vulnerable to the meteorological droughts and water shortages. So, vegetation cover rapidly responds to variation in water availability (Schwinning and Sala, 2004). Thus, more attention should be paid to LULC types in drought studies and planning policies.

The eastern half of the province had a higher correlation (R^2) between meteorological fluctuations and vegetation cover. This is supported by Manesh et al. (2019) who found that vegetation cover is more vulnerable to climate fluctuations in this part of Khorasan Razavi province.

In the study area, 6-month SPEI showed a higher correlation

Table 3. The proportion of the effect of 3, 6 and 12-month SPEI and SPI on different LULC types (%).

LULC Type	SPEI			SPI		
	3-month	6-month	12-month	3-month	6-month	12-month
Dense Forest	10.50	20.97	10.75	16.46	11.00	30.32
Moderate Forest	30.99	21.76	0.22	14.21	24.48	8.34
Sparse Forest	12.00	4.54	6.11	30.52	10.16	36.67
Good Rangeland	24.31	21.70	1.97	18.42	16.73	16.87
Moderate Rangeland	17.41	22.18	4.63	24.03	10.70	21.05
Poor Rangeland	10.08	21.89	7.86	10.49	16.79	32.89
Agricultural Land	20.61	27.15	8.28	17.40	14.07	12.49
Total Area	15.11	23.07	7.14	16.30	14.30	24.08

Table 4. R^2 and regression coefficent (b value) between SVI and multitemporal SPEI and SPI in different LULC types.

LULC Type	R^2	SD	b value	SD
Dense Forest	0.40	0.18	0.81	0.39
Moderate Forest	0.60	0.10	1.13	0.44
Sparse Forest	0.51	0.17	1.03	0.42
Good Rangeland	0.55	0.15	1.01	0.38
Moderate Rangeland	0.48	0.17	0.92	0.40
Poor Rangeland	0.44	0.16	0.85	0.37
Agricultural Land	0.37	0.19	0.75	0.37
Total Area	0.44	0.16	0.85	0.37

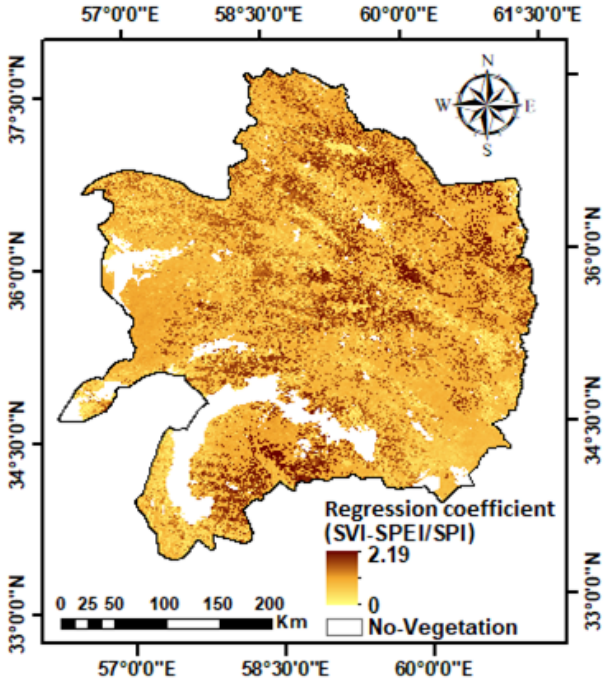

Figure 10. The absolute value of the regression coefficient between SVI and multitemporal SPEI and SPI.

with SVI than other time scales. It should be noted that the SPEI is a common drought index that has the ability to combine precipitation and evaporation and transpiration and is one of the essential factors for estimating crop development and water surplus or deficit evaluation (Ndayiragije and Li, 2022). Agricultural drought was observed in 3 and 6-month time scales while according to Potop et al. (2014), 6 and 12-month time scales are related to the hydrological drought, which is useful for monitoring water resources. Moreover, Shi et al. (2021) reported that the correlation between vegetation cover and meteorological factors are at high level in short or medium time scales in arid and semi- arid regions.

12-month SPI showed the highest correlation in dense forest, sparse forest, and poor rangeland. In fact, the impact of meteorological drought on the vegetation cover in these LULC types has occurred in longer time scales. It is important to mention that the water deficit of the previous months accumulated during SPEI calculation with longer time scales is an indicator to evaluate the moisture deficit, which has caused meteorological and agricultural droughts. The consequence of this also leads to the aggravation of hydrological drought and the reduction of water resources. In contrast, 3-month SPEI had the lowest correlation in moderate forest and good rangeland. Generally, it is inferred that different vegetation communities show different responses to meteorological drought with different time scales. The importance of this issue is highlighted in the study of Entezari et al. (2019). They introduced the knowledge of quantitative and qualitative characteristics of land use changes as valuable for environmental planning, land use and sustainable development.

It was found that vegetation cover in the northeastern and southwestern parts of Khorasan Razavi province is more affected by meteorological drought. Also, the regression coefficient of SVI changes compared to multitemporal SPEI and SPI had different sensitivities in different regions. Since the most sensitive areas are more susceptible to the negative effects of meteorological drought on vegetation, it is necessary that areas with high sensitivity or affected by drought should be prioritized in planning to deal with or reduce the effects of drought and preserve water resources. As it was determined through the correlation values, the highest (R^2 = 0.60) and lowest (R^2 = 0.37) correlations of SVI with multitemporal SPEI and SPI were observed in moderate forest and agriculture. However, these meteorological droughts affect vegetation cover in different ways such as water scarcity, and crop destruction (Poornima et al., 2023). Despite the fact that agricultural lands rely on various meteorological factors such as precipitation, temperature, humidity, etc. for the successful growth of crops, however, the sensitivity of agricultural land compared to other LULC types to meteorological drought changes related to human activities including land management and irrigation. So, in agricultural areas, the possibility of vegetation activity is provided throughout the year.

Finally, according to the findings of this study, SPEI and SPI, as two meteorological indices, had diverse effects on different vegetation types. Thus, any types of indicators should be separately considered in analyzing the response of vegetation cover to climatic variations in terrestrial ecosystems in order to better identify areas affected by meteorological droughts.

Authors contributions
All the authors have participated sufficiently in the intellectual content, conception and design of this work or the analysis and interpretation of the data (when applicable), as well as the writing of the manuscript.

Availability of data and materials
The data that support the findings of this study are available from the corresponding author upon reasonable request.

Conflict of interests
The authors declare that they have no known competing financial interests or personal relationships that could have appeared to influence the work reported in this paper.

References

Adedeji O., Olusola A., James G., Shaba H. A., Orimoloye I. R., Singh S.K., Adelabu S. (2020) Early warning systems development for agricultural drought assessment in Nigeria. *Environmental Monitoring and Assessment* 192 (12): 1–21.

Alamdarloo E. Heydari, Khosravi H., Rahimabadi P. Dehghan, Ghodsi M. (2021) The Effect of Climate Fluctuations on Vegetation Dynamics in West and Northwest of Iran. *Desert Ecosystem Engineering Journal* 3 (2): 19–28.

Allen C. D., Macalady A. K., Chenchouni H., Bachelet D., McDowell N., Vennetier M., Kitzberger T., et al. (2010) A global overview of drought and heat-induced tree mortality reveals emerging climate change risks for forests. *Forest Ecology and Management* 259 (4): 660–684.

Ariapour A., Sabzevar A. Dadrasi, Toloee S. (2013) Estimation of vegetation and land use changes using remote sensing techniques and geographical information system (Case study: Roodab Plain, Sabzevar city). *Journal of Rangeland Science* 4 (1): 1–13.

Entezari A., Zandi R., Khosravian M. (2019) Evaluation of spatial variations of vegetation and surface temperature using Landsat and midsize images, case study: Fars Province, 1967-2017. *Watershed Engineering and Management* 11 (4): 929–940.

Erfanian M., Alizadeh A. (2009) Drought assessment in Khorasan Razavi Province. *Journal of Geography and Regional Development* 13:1–17.

Ezzine H., Bouziane A., Ouazar D. (2014) Seasonal comparisons of meteorological and agricultural drought indices in Morocco using open short time-series data. *International Journal of Applied Earth Observation and Geoinformation* 26:36–48.

Garroutte E. L., Hansen A. J., Lawrence R. L. (2016) Using NDVI and EVI to map spatiotemporal variation in the biomass and quality of forage for migratory elk in the Greater Yellowstone Ecosystem. *Remote Sensing* 8 (5): 1–25.

Ghazaryan G., Dubovyk O., Graw V., Kussul N., Schellberg J. (2020) Local-scale agricultural drought monitoring with satellite-based multi-sensor time-series. *GIScience & Remote Sensing* 57 (5): 704–718.

Huete A., Didan K., Miura T., Rodriguez E. P., Gao X., Ferreira L. G. (2002) Overview of the radiometric and biophysical performance of the MODIS vegetation indices. *Remote Sensing of Environment* 83 (1-2): 195–213.

Iglesias A., Cancelliere A., Wilhite D. A., Garrote L., Cubillo F. (2009) Coping with drought risk in agriculture and water supply systems: Drought management and policy development in the Mediterranean . *Dordrecht, the Netherland: Springer Netherlands* 26

Kendall M. (1975) Rank correlation measures. *Charles Griffin, London* 202:15.

Khusfi Z. Ebrahimi, Zarei M. (2020) Relationships between meteorological drought and vegetation degradation using satellite and climatic data in a semi-arid environment in Markazi province Iran. *Journal of Rangeland Science* 10 (2): 204–217.

Liu Z., Yao Z., Huang H., Wu S., Liu G. (2014) Land use and climate changes and their impacts on runoff in the Yarlung Zangbo river basin, China. *Land Degradation and Development* 25 (3): 203–215.

Manesh M. Behrang, Khosravi H., Alamdarloo E. Heydari, Alekasir M. Saadi, Gholami A., Singh V. P. (2019) Linkage of agricultural drought with meteorological drought in different climates of Iran. *Theoretical and Applied Climatology* 138:1025–1033.

Mann H. B. (1945) Nonparametric tests against trend. *Econometrica: Journal of the Econometric Society* 13 (3): 245–259. https://doi.org/10.2307/1907187

Matsushita B., Yang W., Chen J., Onda Y., Qiu G. (2007) Sensitivity of the enhanced vegetation index (EVI) and normalized difference vegetation index (NDVI) to topographic effects: a case study in high-density cypress forest. *Sensors* 7 (11): 2636–2651.

McKee T. B., Doesken N. J., Kleist J. (1993) The relationship of drought frequency and duration to time scales. *In Proceedings of the 8th Conference on Applied Climatology, Boston, MA, USA, January* 17-22:179–184.

Miao L., Ye P., He B., Chen L., Cui X. (2015) Future climate impact on the desertification in the dry land Asia using AVHRR GIMMS NDVI3g data. *Remote Sensing* 7:3863–3877.

Ndayiragije J. M., Li F. (2022) Monitoring and analysis of drought characteristics based on climate change in Burundi using standardized precipitation evapotranspiration index. *Water* 14 (16): 1–19.

Ozelkan E., Chen G., Ustundag B. B. (2016) Multiscale object-based drought monitoring and comparison in rainfed and irrigated agriculture from Landsat 8 OLI imagery. *International Journal of Applied Earth Observation and Geoinformation* 44:159–170.

Pakeman R. J., Fielding D. A., Everts L., Littlewood N. A. (2019) Long-term impacts of changed grazing regimes on the vegetation of heterogeneous upland grasslands. *Journal of Applied Ecology* 56:1794–1805.

Pogacar T., Znidarsic Z., Vlahovic Z., Crepinsek Z., Susnik A. (2022) Grassland Model Based Evaluation of Drought Indices: A Case Study from the Slovenian Alpine Region. *Agronomy* 12 (4): 1–18.

Poornima S., Pushpalatha M., Jana R. B., Patti L. A. (2023) Rainfall Forecast and Drought Analysis for Recent and Forthcoming Years in India. *Water* 15 (3): 1–17.

Potop V., Boroneanţ C., Mozny M., Stepánek P., Skalák P. (2014) Observed spatiotemporal characteristics of drought on various time scales over the Czech Republic. *Theoretical and Applied Climatology* 115:563–581.

Schwinning S., Sala O. E. (2004) Hierarchy of responses to resource pulses in arid and semi-arid ecosystems. *Oecologia* 141:211–220.

Shad M. Safari, Ildoromi A., Akhzari D. (2017) Drought monitoring using vegetation indices and MODIS data (case study: Isfahan province, Iran). *Journal of Rangeland Science* 7 (2): 148–159.

Shi S., Yu J., Wang F., Wang P., Zhang Y., Jin K. (2021) Quantitative contributions of climate change and human activities to vegetation changes over multiple time scales on the Loess Plateau. *Science of The Total Environment* 755:1–50.

Su Z., He Y., Dong X., Wang L. (2017) Remote Sensing of Hydrological Extremes. *Remote Sensing of Hydrological Extremes,* 151–172.

Tarnavsky E., Bonifacio R. (2020) Drought risk management using satellite-based rainfall estimates. *Satellite Precipitation Measurement* 2:1029–1053.

Thornthwaite C. W. (1948) An approach toward a rational classification of climate. *Geographical Review* 38 (1): 55–94.

Tsakiris G., Vangelis H. (2004) Towards a Drought Watch System based on spatial SPI. *Water Resources Management* 18 (1): 1–12.

Veneros J., García L. (2022) Application of the Standardized Vegetation Index (SVI) and Google Earth Engine (GEE) for drought management in Peru. *Tropical and Subtropical Agroecosystems* 27:1–13.

Vicente-Serrano S. M., Beguería S., López-Moreno J. I. (2010) A multiscalar drought index sensitive to global warming: the standardized precipitation evapotranspiration index. *Journal of Climate* 23 (7): 1696–1718.

Vicente-Serrano S. M., Gouveia C., Camarero J. J., Beguería S., Trigo R., López-Moreno J. I., Azorín-Molina C., et al. (2013) Response of vegetation to drought time-scales across global land biomes. *Proceedings of the National Academy of Sciences* 110 (1): 52–57.

Wei Y., Zhu L., Chen Y., Cao X., Yu H. (2022) Spatiotemporal Variations in Drought and Vegetation Response in Inner Mongolia from 1982 to 2019. *Remote Sensing* 14 (15): 3803.

West H., Quinn N., Horswell M. (2019) Remote sensing for drought monitoring & impact assessment: Progress, past challenges and future opportunities. *Remote Sensing of Environment* 232:111291.

Williams C. A., Albertson J. D. (2006) Dynamical effects of the statistical structure of annual rainfall on dryland vegetation. *Global Change Biology* 12:777–792.

Zandi R., Entezari A., Baaghide M., Khosravian M. (2021) Evaluation of drought and its effects on vegetation in southern regions of Iran. *Researches in Earth Sciences* 12 (2): 36–49. https://doi.org/InPersian

Zargar A., Sadiq R., Naser B., Khan F. I. (2011) A review of drought indices. *Environmental Reviews* 19 (1): 333–349.